ME-86-06

The Effect of Microclimate on the Deterioration of Concrete Barrier Walls

Ontario Ministry of Transportation and Communications
Research and Development Branch

Technical Report Documentation Page

The Effect of Microclimate on the Deterioration of Concrete Barrier Walls

Author:	**P.P. Hudec, C. MacInnis, M. Moukwa** University of Windsor
MTC No.:	ME-86-06
Date:	October 1986
Others:	
Published by:	The Research and Development Branch Ontario Ministry of Transportation and Communications
Participating Agencies/-Client:	
Abstract:	The south facing vertical surfaces of concrete barrier walls often exhibit considerable scaling which suggests that such surfaces are subjected to more severe exposure conditions. The objective of this research was to determine and define the microclimate by measuring the temperature and moisture conditions obtained at the surface and near the sub-surface of the south and north facing barrier walls. A method was developed to determine moisture (and to some extent, salt) content of the concrete by measuring the change in capacitance of the concrete when an electric current was passed through it. Temperature was measured by thermocouples embedded at the surface and at a depth of 1 cm. Two field exposure sites were included in the study: a south facing wall on E. C. Row Expressway in Windsor, Ontario, and two laboratory-cast barrier wall panels placed to face south and north respectively on the roof of Essex Hall on the campus of the University of Windsor. The field measurements of temperature and apparent capacitance were obtained on a semi-continuous basis for the months of January, February and March, 1984. The results indicate that the south-facing walls undergo a significantly greater number of freezing and thawing cycles than north-facing walls. The temperature gradient of over 10°C between the surface and a 1 cm depth was common. The rate of freezing and thawing was significantly higher on the south-facing wall than on the north-facing wall. Because of greater insolation, the south-facing wall experienced a greater number of drying and wetting cycles and also tended to be above "critical" saturation levels relatively frequently.
Key words	concrete deterioration, microclimate, barrier walls, concrete moisture content, concrete temperature, concrete durability
Comments:	Final report of Research and Development Branch Project No. 221125, conducted under the *Ontario Joint Transportation and Communications Research Program.*
Distribution:	MTC Head Office and Regions, engineers involved with concrete design and rehabilitation.
Copyright Status:	Crown copyright

ME-86-06

The Effect of Microclimate on the Deterioration of Concrete Barrier Walls

P.P. Hudec

C. MacInnis

M. Moukwa

University of Windsor

Published by
The Research and Development Branch
Ontario Ministry of Transportation and Communications
Hon. Ed Fulton, Minister
D.G. Hobbs, Deputy Minister

Published without prejudice as to the application of the findings. Crown copyright reserved; however, this document may be reproduced for non-commercial purposes with attribution to the Ministry.

For additional copies, contact:
The Editor, Technical Publications
Ministry of Transportation and Communications
1201 Wilson Avenue
Downsview, Ontario
Canada M3M 1J8

Telephone: (416) 248-7226
Infotex electronic mail: 21: MIN006

October 1986

Table of Contents

List of Tables v
List of Figures vi

1/ Introduction 2

2/ The Capacitance Effect for Moisture and Salt Determination 3
2.1/ Theoretical Considerations 4

3/ Laboratory Studies 5
3.1/ Specimen Preparation 5
3.2/ Capacitance Measurements on Laboratory Samples 5
3.2.1/ Effect of Water-Cement Ratio 6
3.2.2/ Effect of Aggregates 6
3.2.3/ Effect of Salts 6
3.2.4/ Effect of Temperature 6
3.2.2/ Effect of Aggregates
3.3/ Salt Content of Mortar and Concrete Specimens 7
3.4/ Moisture and Concrete Determination from Capacitance Data 7
3.4.1/ Statistical Evaluation of Temperature Effect 7
3.4.2/ Statistical Evaluation of the Capacitance Effect 7
3.4.3/ Salt Content "Range" Calculations 9

4/ Field Studies 9
4.1/ E.C. Row Expressway Panels 9
4.2/ Roof Panels 10
4.3/ Laboratory Specimens 10
4.4/ Moisture and Salt Content of the Panels by Direct Analysis 10
4.5/ Temperature and Current Readings and Snow Conditions 11

5/ Data Analysis 11
5.1/ Daily Temperature Variations – Roof Panels 11
5.2/ Daily Temperature Variations – E.C. Row Panels 11
5.3/ Rates of Temperature Change – E.C. Row Panels 12
5.4/ Freezing and Thawing Cycles 13
5.5/ Temperature Changes at the Snow Line 14
5.6/ Moisture and Salt Content of the Panels 14
5.7/ Degree of Saturation of the Panels 14
5.7.1/ Effect of Panel Orientation on Moisture Content 14
5.8/ Salt Content in the Panels 15
5.9/ Freezing and Moisture Content 15

6/ Conclusions and Recommendations 16

References 17

List of Tables

3.1/ Results of Chloride Analysis for Concrete of Composition E 18

3.2/ Multiple Linear Regression Model for Compositions A and B 19

3.3/ Regression Analysis Model for Salt Content Prediction 20

3.4/ Calculated Salt Content Categories 21

4.1/ Current and Moisture Data from the Samples Chiseled from the Roof and E.C. Row Panels 22

5.2/ Frequency of Temperature Change in the E.C. Row Panel for the Month of March 23

5.3/ Cooling and Warming Rate Frequency (in %) for the Period of March 4 to March 24, E.C. Row Panel 24

5.4/ Average Degree of Saturation for the Roof Panels 25

5.5/ Categories of Salt Content for the Bottom Part of E.C. Row Panel 26

5.6/ Average Degree of Saturation for the North and South Facing Roof Panels 27

5.7/ Salt Content Categories in the Bottom Part of E.C. Row Panel 28

List of Figures

2.2.1/ Square Wave Generator 29

2.2.2/ Regulated DC Power Source Circuit 29

3.1/ Change of Capacitance with Time for Two W/C 30

3.2/ Effect of Salt on the Capacitance Effect 30

3.3/ Effect of Temperature on the September 20 Reading 31

3.4/ Current Ratio I(T)/I(20) vs Temperature at 100 Hz 31

3.5/ Current at 10 Hz vs Current at 100 Hz, Composition E 32

3.6/ Frequency of Occurrence of Current Readings at 10 Hz for Three Ranges of Degree of Saturation 33

4.1/ General View of the E.C. Row Site 33

4.2/ Location of the Thermocouples in the E.C. Row Panels 34

4.3/ General View of the Roof Installation 34

4.4/ Schematic Diagram Showing How the Roof Panel was Sprayed With a Salt Solution 35

5.1/ Typical Temperature Variation in the Roof's South Facing Panel for a Sunny, Cold Day 35

5.2/ Typical Temperature Variation in the Roof's South Facing Panel for a Sunny, Warm Day 36

5.3/ Typical Temperature Variation in the Roof's South Facing Panel for a Partly Sunny, Cold Day 36

5.4/ Typical Temperature Variation in the Roof's South Facing Panel for a Cloudy, Cold Day 37

5.5/ Temperature Distribution in Panel East (E.C. Row), from January 21 to January 26, 1984 37

5.6/ Temperature Distribution in Panel East (E.C. Row), from January 31 to February 6, 1984 38

5.7/ Daily Temperature Variation for Panel West (E.C. Row) on February 25, 1984 38

5.8/ Daily Temperature Variation for Panel West (E.C. Row) on February 23, 1984 39

5.9/ Daily Temperature Variation for Panel West on March 2, 1984 39

5.10/ Daily Temperature Variation for Panel West on March 8, 1984 40

5.11/ Typical Daily Change in Δ T for February 25, 1984 40

5.12/ Typical Daily Change in Δ T for March 7, 1984 41

5.13/ Number of Freezing and Thawing Cycles Per Day for all the Thermocouples 41

5.14/ Frequency of Freezing Rate for Thermocouples 1, 9, 5, and 13, for the Month of March 42

5.15/ Temperature Distribution in Panel East Installed on E.C. Row, from January 21 to January 26, 1984 43

5.16/ Temperature Distribution in Panel East Installed on E.C. Row, from January 31 to February 6, 1984 43

MICROCLIMATE OF CONCRETE BARRIER WALL: TEMPERATURE, MOISTURE AND SALT CONTENT

By:

Peter P. Hudec, Ph.D., P.Geol.

Cameron MacInnis, Ph.D., P.Eng.

Mosongo Moukwa, M.A.Sc.

University of Windsor, Windsor, Ont.

ABSTRACT

The south facing vertical surfaces of concrete barrier walls often exhibit considerable scaling which suggests that such surfaces are subjected to more severe exposure conditions. The objective of this research was to determine and define the microclimate by measuring the temperature and moisture conditions obtaining at the surface and near sub-surface of south and north facing barrier walls.

A method was developed to determine moisture (and to some extent, salt) content of the concrete by measuring the change in capacitance of the concrete when an electric current was passed through it. Temperature was measured by thermocouples embedded at the surface and at the 1 cm depth. Two field exposure sites were included in the study: a south facing wall on E.C. Row Expressway in Windsor, Ontario, and two laboratory cast barrier wall panels placed to face south and north respectively on the roof of Essex Hall on the campus of the University of Windsor. The field measurements of temperature and apparent capacitance were obtained on a semi-continuous basis for the months of January, February, and March, 1984.

Statistical predictive models of moisture content based on capacitance effect measurements of lab samples were developed, and applied to field measurements. Temperature data were statistically evaluated to determine temperature extremes, gradients, and frequency of freezing and thawing cycles.

The results indicate that the south-facing walls undergo a significantly greater number of freezing and thawing cycles then north-facing walls. A temperature gradient of over 10C between surface and the 1 cm depth was common. Rate of freezing and thawing was sig-

nificantly higher on the south facing wall then on the north facing wall. The south facing wall experienced a greater number of drying and wetting cycles, and also tended to be above "critical" saturation levels relatively frequently.

All of the above conditions indicate that a much greater severity of microclimate exists on south facing walls. This can be attributed directly to greater insolation received by the walls.

1.0 INTRODUCTION

Some concrete barrier walls, commonly used along Ontario highways and elsewhere, have shown unexpectedly rapid deterioration in the form of surface scaling. Typically the deterioration has tended to be more pronounced on the south-facing walls. Observation of walls during the winter months suggests that there is a substantial difference in the microclimate of south facing walls. Often as a result of winter maintenance operations, the face of the wall is covered in hardpacked snow, containing deicing salt. The upper vertical face of a wall may be free from snow, but can be wet from the melting snow on the top of the wall. Water has been recorded running down the face of such walls at temperatures as low as -15C. It is believed that such concrete is exposed to a much more severe exposure condition than concrete of other orientations and that this is responsible for the more pronounced scaling sometimes observed.

Research, funded by the Ontario Ministry of Transportation and Communications (MTC) under OJT and CRP Project 22125, was undertaken to determine the microclimate at such walls. The microclimate elements to be measured were temperature at the surface and near subsurface, moisture content, and salt content.

The measurement of temperature presented no problem. Standard copper-constantan thermocouples embedded in the surface and near subsurface were used. However, the measurement of moisture and salt content required an indirect sensing technique, since physical samples could be taken only infrequently, and then only for calibration purposes.

A number of techniques were considered. The method selected relies on the determination of the electrical capacitance effect. Rather than measuring capacitance directly, changes in capacitance at two frequencies - 10 and 100 MHz - were determined. The capacitance

of concrete is related to its resistivity (or conductivity), which in turn is related to moisture content and the amount of dissolved salts. It was thus hoped that changes in capacitance would be related to changes in moisture and salt content of the concrete surface.

The first phase of the research was carried out in the laboratory on cement paste, mortar, and small concrete specimens. Small, portable, low-power, electronic instrumentation was designed and built which allowed the measurement of the capacitance effect using stainless steel electrodes embedded in the specimens. Moisture content of the specimens was determined gravimetrically, and salt content by chemical analysis. The results were related to the measured capacitance effect.

Statistical comparisons showed that a good and reproducible relationship exists between moisture and the capacitance effect. A less well defined relationship was found between the salt content and the capacitance effect.

Two field sites were chosen for monitoring the microclimate conditions present on and in surface layers of full-sized barrier walls. One site was an existing south facing barrier wall along a heavily traveled divided four-lane highway in South Windsor, the E.C. Row Expressway. The other site chosen was the roof of Essex Hall on the campus of the University of Windsor, for which two concrete barrier wall sections were cast and instrumented in the lab, and then placed on the roof in north- and south- facing positions respectively.

The details of the laboratory tests, field installation, and the treatment and discussion of the results are given in a report on file with MTC. What follows is a summary report of the procedures and results.

2.0 THE CAPACITANCE EFFECT FOR MOISTURE AND SALT DETERMINATION

Water changes not only the electrical condition but also the dielectric properties of concrete.

According to Bell, Leonards and Dolch (1), the dielectric constant and the capacitance of concrete increase with water content. Thus by measuring the change in the capacitance it was postulated that it should be possible to determine the amount of water present in concrete specimens. The effect of salt content on capacitance was not known.

The electrical properties of concrete can be measured through electrodes embedded at short intervals. In this case, the electrodes consisted of stainless steel rods which were insulated with "shrink fit" tubing and embedded approximately 1 cm apart and 1 cm deep.

2.1 THEORETICAL CONSIDERATIONS

A block of concrete or mortar with embedded electrodes can be considered as a complex network of resistance and capacitance. Each path of the A.C current can be represented by a parallel circuit of resistor and capacitor as shown in Figure 2.1.

It can be assumed that at low frequency (10Hz) the total current passes through the resistance since the capacitive reactance is very high for that condition. The resistance can therefore be calculated by assuming D.C current. At high frequencies the model can be expressed as a single capacitance C connected in parallel with a resistance.

The equivalent circuit for the conductive path between the electrodes is shown in Figure 2. When a square wave generator is used to excite the circuit, the resultant currents can be computed using impedance concepts associated with steady-state sinusoidal analysis. This is possible since a symmetrical square wave with a peak value of Vm and having an average value of zero can be expressed as a Fourier series with the form

$$v(t) = \sum_{n=1}^{n=\infty} (4\ Vm / \pi\ n) \sin n\ \omega\ t, \quad n= 1,3,5,....2p+1,...$$

where ω is the frequency in radians per second, t is time in seconds, p is an integer, and n is the order of the harmonic, with n+1 called the fundamental frequency.

For the circuit in Figure 2 the sum of the branch currents or total current for the n-th order harmonic is given by

$$Im = \frac{4\ Vm}{n} \left[\frac{1}{R_1} \quad \frac{j}{1/n\omega C_1} \quad \frac{1}{R_2 - j(1/n\omega C_2)} \right]$$

where Im is the peak value of the current phasor. The total R.M.S. current supplied by the generator is given by

$$I_T\ (RMS) = \sqrt{1/2 \sum_{n=1}^{n=\infty} I\ n^2} \qquad (n \text{ odd})$$

It is the "capacitance effect" and its change which are measured, not the absolute capacitance. However for our purposes, we need to know only how changes in capacitance are affected by changes in the moisture and salt content of the specimen.

2.2 EQUIPMENT

The equipment consisted of a portable current generator, and a digital multimeter. The generator is capable of producing a square wave alternating current and voltage at two frequencies 10Hz and 100Hz. The circuit diagram of the power source is shown in Figure 2.2. The measurements were obtained by applying a constant electric voltage between the two embedded electrodes and measuring the resulting current at 10Hz and 100Hz, using a digital multimeter.

3.0 LABORATORY STUDIES

3.1 SPECIMEN PREPARATION

An experimental laboratory testing programme was designed to investigate the "capacitance effect" for different moisture contents of mortars and concrete mixtures, and to derive capacitance-moisture and capacitance-salt content relationships.

Pilot studies were conducted with four different compositions of mortar and two different compositions of concrete. The compositions varied in coarse/fine aggregate ratio, water/cement ratio, and air contents. Based on the results obtained, one composition of concrete was chosen for field studies: Type 10 cement, W/C = 0.47, C:F.A.:C.A = 1:1.4:1.6, entrained air = 7 percent.

The concrete specimens were cast (with electrodes in place) as a single panel, which was cured in the mold under wet burlap for one day, and then taken from the mold and immersed in water for 7 days. Specimens approximately 3 x 1.5 x 2 cm were then cut from the panel. All cutting was done wet. Each specimen contained two insulated electrodes 1cm apart and 1 cm deep, with tips exposed.

The mortar specimens were cast in individual molds, also with embedded electrodes in place. The specimens were 2 x 2.5 x 3 cm in size.

3.2 CAPACITANCE MEASUREMENTS ON LABORATORY SAMPLES:

The capacitance effect was determined first on saturated, surface dry specimens; the specimens were then partly dried and new determina-

tions were made at the lower water content. In this way several different moisture conditions were obtained. The moisture content was determined relative to the saturated surface-dry condition. The driest condition for the specimens was produced by oven drying at 50C.

3.2.1 EFFECT OF WATER - CEMENT RATIO

The water-cement ratio determines the total porosity and concentration of ions in the pore water solution. It also controls the electrical properties of the concrete. The effect of water-cement ratio on the capacitance is shown in Figure 3.1. Compositions II and III have water-cement ratios of 0.43 and 0.47 respectively. The figure also shows that the capacitance was reduced with time for continuous moist storage. After 28 days there was no detectable change in the electrical properties. Decrease of evaporable water with continuing hydration is one possible factor, but other effects such as continuing release of alkalis and leaching can also influence the capacitance.

3.2.2 EFFECT OF AGGREGATES

Tests conducted by Whittington, Mac Carter and Forde (4) showed that concrete can be considered as a composite of non-conductive particles contained in a conductive cement paste matrix. The resistivities of the aggregates are much higher than those of concrete. Thus a high proportion of the current passes through the cement paste. The aggregate used in our experimental work was dolomite and dolomitic limestone.

3.2.3 EFFECT OF SALTS

Spencer (2) found that the conductivity of concrete was strongly influenced by dissolved salts. Bell, Leonards and Dolch (1) also found that the dielectric properties of concrete were sensitive to increases in the salt concentrations of pore water.

The effect of dissolved salt on the capacitance effect and current for a specimen soaked in a 3% salt solution for 1 day is shown in Figure 3.2.

3.2.4 EFFECT OF TEMPERATURE

The effect of elevated temperatures on the electrical properties of concrete has been mentioned by some researchers (2,3,4). However, little work has been done on the effect of low temperatures. A test was performed using 20 specimens. The temperatures at which the readings were taken were 15.5C, 10C, 4.4C, -1.1C, -6.6C and -12C.

Figure 3.3 shows the effect of temperature on concrete resistance for different degrees of saturation. The resistance was reduced with temperature.

3.3 SALT CONTENT OF MORTAR AND CONCRETE SPECIMENS

The most popular method of chloride analysis is Volhard's method. In the procedure developed by Berman which is based on Volhard's method, the total quantity of chloride in hardened concrete is determined by dissolving approximately 4g of the ground sample in HNO_3, then filtering and titrating with 0.01N $AgNO_3$ using chloride electrode. The accuracy of the method is within 0.5% of the chloride present (5). This procedure has been recommended by the Ontario Ministry of Transportation and Communications (MTC) and was followed in this work.

Tests showed that a composite sample, taken from several specimens saturated in the same salt solution can be used as a representative sample for chloride content. The composite samples were prepared as follows: from a population of laboratory samples at each salt concentration 3 specimens were selected randomly and pulverized. Four grams of each composite sample were taken for analysis. The results of analysis are given in Table 3.1.

The chloride content of the field panels after one winter's exposure was determined from chiseled-out samples.

3.4 MOISTURE AND SALT CONTENT DETERMINATION FROM CAPACITANCE DATA

Although it has been reasonably well established that the current is affected by the moisture and salt content of the concrete, the exact relationship between the capacitance effect and these parameters needed to be developed. To this end, a statistical regression model was evolved that predicts the degree of saturation in concrete from the current readings at 10Hz and 100Hz. However, there was no statistical correspondence found between current readings and salt content; only approximate ranges of salt concentrations present could be predicted.

3.4.1 STATISTICAL EVALUATION OF TEMPERATURE EFFECT

Simple linear correlation and regression analysis between the current and temperature was performed. The regression lines shown in Figures 3.4 is represented by the following equation:

$$R100 = 0.5089 + (0.02158)\ TEMP$$

where R100 is the average current at 100Hz; TEMP is the concrete tem-

perature at the time of the reading. Correlation for the above relationship was highly significant.

3.4.2 STATISTICAL EVALUATION OF THE CAPACITANCE EFFECT

The current readings at 10Hz and 100Hz, the calculated capacitance effect, and the moisture content and salt content data were statistically evaluated. The data from concrete of two similar compositions (A & B) were used, comprising 4629 individual readings. There is an excellent correlation between the currents and the calculated capacitance effect, and also between these measurements and the moisture content. A significant, but much poorer correlation was found to exist between the electrical measurements and the salt content. Considered individually, the two compositions gave almost identical results.

A stepwise regression analysis was carried out in which the moisture content and the salt content were the dependent variables, and the current readings, capacitance effect, resistivity, and their log equivalents were the independent variables. The intent of the statistic was to build a mathematical model that would enable the calculation of moisture and salt contents from the electrical data.

The stepwise linear regression model that predicts the degree of saturation for combined compositions A and B is given in Table 3.2. The salt content was shown to have low linear and log correlation with the electrical properties. Nevertheless, a stepwise regression analysis was attempted, and the results are given in Table 3.3.

The models so derived were used to predict (calculate) the moisture and salt contents. The predicted and the actual moisture and salt contents were compared by the t-statistic. It was found that there was no difference between the calculated and actual moisture contents at the 99% confidence level. However, using the same procedure, it was determined that there was a significant difference between the means of salt contents at 95% confidence level. It would thus appear that the moisture content (degree of saturation) can be confidently predicted using the capacitance effect measurements, but the salt content cannot be determined by these measurements directly.

However, when current measurements at 10Hz and 100Hz are plotted with salt content numbers used as points, it is seen that they tend to

cluster and increase as the current readings increase (Figure 3.5). Thus it is possible to obtain approximate ranges of salt content.

3.4.3 SALT CONTENT "RANGE" CALCULATIONS

Examination of Figure 3.5 shows that the salt content can be obtained within a certain range for a given pair of currents (at 10Hz and at 100Hz). However, the degree of saturation has not been taken into account. The same current generated in a sample at 40% saturation with a 9% salt solution can also be obtained with a specimen fully saturated with a 3% salt solution. Current readings less than 0.2 mA were obtained only with a low degree of saturation.

Ranges of probable salt content for a given degree of saturation were defined by the following procedure:

Samples were divided into nine salt content ranges. For each salt content range, three ranges of the degree of saturation were defined. The frequency of occurrence of a given current value was calculated for each degree of saturation range. The results are given in Figure 3.6. Ten classes of currents intensities were defined and are reported in Table 3.4.

4.0 FIELD STUDIES

After the techniques of indirectly measuring moisture and salt content of specimens were established, field panels were cast and instrumented for the two outdoor exposure sites. In addition to the panels a number of small laboratory specimens (1x1x2 cm) with embedded electrodes were prepared from the same mixture for moisture and salt calibration purposes.

4.1 E.C. ROW EXPRESSWAY PANELS

Two test panels were installed on site 06 - 287 of the E.C. Row Expressway. The panels were installed on an existing section of barrier wall adjacent to a railroad overpass. The overpass provided a convenient location for temperature monitoring equipment (Figure 4.1).

A 70 cm width (28") of concrete was removed to a depth of 5 cm (2") from the surface of an existing barrier wall as shown in Figure 4.2. The space so created was filled with new concrete in which thermocouples and electrodes were installed. A wide section of concrete was left between the two sets of electrodes to enable the chiseling out of pieces of concrete for direct moisture and salt determination.

Two sets of electrodes were installed in the panels at 1 cm spac-

ings and to a depth of 1 cm. To allow the moisture content to be monitored at the surface and at the 1 cm depth, each alternate pair had either the tips or the surface section insulated.

The thermocouples used were of copper-constantan type and were placed in the panels as shown in Figure 4.2:

Panel I - 8 on the surface
and - 8 at 1 cm depth
Panel II - 2 at 5 cm depth in Panel I
- 2 at 3 cm depth in Panel II
- 1 in the air.

The thermocouples were wired to two 10-channel signal scanners. A battery operated chart recorder was used to record the temperatures read by the temperature sensors. Two kerosene lamps were used to keep the instruments from freezing.

4.2 ROOF PANELS

Two test panels having the shape and dimensions of barrier walls and two feet in length were cast in the laboratory. The concrete was essentially of the same composition as that used at the E.C. Row site. The panels were cured for one month in the laboratory before they were moved to the roof of the Engineering building (Essex Hall, University of Windsor campus) on February 3, 1984. One was placed facing south and the other facing north. Figure 4.3 shows the general view of the roof installation.

Electrodes and thermocouples were installed in the panels in the same manner indicated for those at the E.C. Row site. Salt was artifically introduced into the roof panels by repeated spraying of selected zones of the panels with a 9% NaCl solution. The method of spraying is given in Figure 4.4. Current readings were taken after each spraying.

4.3 LABORATORY SPECIMENS

Concrete specimens* were cast as a single panel (50 x 80 x 10 cm) with the electrodes embedded. Specimens approximately 3 x 1.5 x 2 cm were then sawn from the panel. The specimens were used as lab control for the field sites. Tests were performed on the lab control specimens in the manner described for the pilot study.

4.4 MOISTURE AND SALT CONTENT OF THE PANELS BY DIRECT ANALYSIS

Samples were chiseled at different locations from the panels installed on the roof and on the E.C. Row site to determine the actual

degree of saturation and salt content. The current readings were also taken. Water content and the degree of saturation was determined and related to the current readings. Salt content was determined chemically. The results are given in Table 4.1.

4.5 TEMPERATURE AND CURRENT READINGS AND SNOW CONDITIONS

Data collection was initiated on the E.C. Row panels on January 8, 1984 and on the roof panels on February 6, 1984. Current readings, temperatures and snow levels were recorded. Due to persistent instrument malfunction it was not possible to obtain continuous 24 hour temperature data during the month of January. However frequent spot temperature readings were taken during this period. From Mid february, sufficient data was collected on a continuous basis for a variety of weather conditions, on both the E.C. Row Panel West and on the roof panels. The outside temperature, relative humidity, wind direction and precipitation were obtained from the Windsor Airport weather station nearby. The sunshine record was not available from the Windsor Airport but was obtained from the nearby Harrow weather station.

The panels installed on the E.C. Row site were at times completely covered with snow and ice. Under such conditions it was impossible to obtain the current measurements at all electrodes. In contrast, the roof panels were never covered with snow, because of the strong winds blowing at the roof level.

5.0 DATA ANALYSIS

5.1 DAILY TEMPERATURE VARIATIONS - ROOF PANELS

Typical daily temperature variation in the roof south facing panel is shown in Figures 5.1 to 5.4 for 4 distinctly different types of weather conditions:

sunny and cold

sunny and warm

partly sunny and cold

cloudy and cold

The above were chosen to illustrate principally the relationship between insolation and ambient temperature on conditions existing at and below the concrete surface.

5.2 DAILY TEMPERATURE VARIATIONS - E.C. ROW PANELS

Snow and ice which covered the E.C. Row barrier walls from time to time has to be taken into account. Snow cover has a pronounced ef-

fect on the concrete temperature, because it protects the concrete surface from solar radiation, wind, and changes in the ambient temperature.

Figures 5.5 and 5.6 show typical concrete temperature distribution in the E.C. Row panel at approximately noon time for the period of January 21 to January 26 and for the period of January 31 to February 6. In these figures the temperature at the surface and at the 1 cm depth are represented. The level of the snow, the type of weather and the outside temperature at the time of the measurement are also indicated.

Figures 5.7 to 5.10 show the daily variation of the concrete temperature for the following conditions:

Fig. 5.7 Sunny and cold day;
Concrete wall not covered with snow.

Fig. 5.8 Sunny and warm day;
Concrete wall not covered with snow.

Fig. 5.9 Partly sunny and cold day;
Concrete wall completely covered with snow.

Fig. 5.10 Cloudy and cold day;
Concrete wall covered half way with snow.

When the barrier walls are not covered with snow the distribution of the concrete temperature is similar to the observation made for the roof panels. When the barrier wall is covered with snow, the concrete temperature is greatly affected. Figure 5.9 shows, for example, that even though March 2 was a sunny day, the concrete temperature at the bottom of the panel did not rise with the air temperature. At times on sunny days, the bottom areas were colder than the top. On the other hand, the roof panels showed that on sunny days the bottom of the panel was usually warmer than the top. On the E.C. Row site snow sometimes protected the concrete wall against wind and solar radiation.

5.3 RATES OF TEMPERATURE CHANGE - E.C. ROW PANELS

The temperature data analysis is presented for the E.C. Row installation only. The roof panels experienced similar temperature fluctuations, and are discussed in the detailed report. The daily rate of change in temperature was calculated for all the thermocouples and the maxima and minima rates are reported in Table 5.1. The frequency of each category of temperature change is reported in Tables

5.2 and 5.3 respectively for February and March.

High temperature gradients were recorded at the bottom of the panel in the months of February and March. A maximum rise of 12.7 C/h was recorded in February, and 14.3 C/h was recorded on March 6. On that day in March the wall was half covered with snow and ice. The rate of temperature change between 0 and 3 C/h occurred more often. The highest recorded changes in the air temperature were only 2.0 and 3.2 C/h on warming and cooling respectively. The largest difference in temperature (dT) between the surface and at 1 cm depth was found to be 10.5 C when the surface was hotter than the inside. This occurred on a partly cloudy day when the wall was free of snow. During the times when the surface was colder than the inside, the maximum recorded difference in temperature was 8.5 C. On that day it was sunny and cold and the wall was half covered with snow.

Typical daily changes in dT experienced at the bottom and at the top of the panel are shown in Figures 5.11 and 5.12 for February 25 and March 7 respectively (sunny and cold days). On February 25 the wall was free of snow whereas on March 7 the wall was covered half way with snow.

5.4 FREEZING AND THAWING CYCLES

The temperature change from above to below the freezing point can be defined as one cycle of freezing and thawing. Because of the pore size considerations, the minimum temperature required to freeze capillary water was taken as -3 C.

The rate of freezing or thawing was determined by the slope of the curve between two consecutive temperature readings. The number of freezing and thawing cycles for the period is reported in Figure 5.13. More freeze-thaw cycles occurred in March because in 1984 March was colder than February.

The rate of freezing was calculated for all the thermocouples and the maxima rates are reported in Figure 5.14 for thermocouples 1, 9, 3 and 11 (bottom) and also for thermocouples 5, 13, 7 and 15 (top) (see Figure 4.2). The rate of freezing and thawing ranged from 0.3 to 12.8 C/h. The maxima rates obtained for the E.C. Row panel were higher than those obtained for the roof panels. At the bottom of the panel freezing proceeds most often at a rate between 6 and 9 C/h. Conversely freezing at the top proceeds most often at the lower rate of between 0 and 3 C/h. Thawing at the top or the bottom of the panel

proceeds most often at a rate between 0 and 3 C/h. It has also been observed that freezing occurs first on the surface and usually a half an hour later at 1 cm depth in the concrete.

5.5 TEMPERATURE CHANGES AT THE SNOW LINE

Concrete can be subjected to significant lateral changes in temperature at the snow line of the barrier wall as shown in Figures 5.15 and 5.16. For instance, on January 25, a difference of 10C was recorded over a distance of 10 cm across the snow line. Such temperature differences can set up significant stresses, which, if repeated can contribute to concrete deterioration.

5.6 MOISTURE AND SALT CONTENT OF THE PANELS

It was established in the laboratory that the two frequencies method can be used to predict the degree of saturation and to some extent, the salt content of the concrete.

The current readings obtained on the panels were first temperature corrected, and then the moisture content (degree of saturation) was calculated. The multiple linear regression model that predicted the degree of saturation was used to calculate the moisture content in the panels.

A t-test was used to compare the degree of saturation obtained directly from the chiseled samples and the calculated results. At a 0.05 level of significance there was no significant difference between them.

The discrepancies between the actual and the predicted degree of saturation can be attributed to:

1. The assumption that the degree of saturation was a linear function of the currents and their logarithms.
2. Poor contact between the electrodes and the surrounding concrete.

5.7 DEGREE OF SATURATION OF THE PANELS

Figures 5.17 shows the degree of saturation in the E.C. Row panel. It is reasonable to assume that near 100% saturation was reached at the bottom of the panel when it was covered with snow. The concrete temperature at different locations is also given.

5.7.1 EFFECT OF PANEL ORIENTATION ON MOISTURE CONTENT

Although moisture content in the barrier walls occasionally fluctuated due to heavy wetting and rapid drying it is obvious that moisture content is affected by the orientation of the panel. As the prevailing wind direction is from the south, the south facing wall

should have higher moisture content as a result of driving rain. On the other hand, the south facing panel will dry faster than the north facing panel. The values of the average degree of saturation calculated for the roof panels at the surface and at 1 cm depth confirm this general observation. These values are reported in Table 5.4.

5.8 SALT CONTENT IN THE PANELS

The probable salt content of the panels was calculated using the frequency - class method described earlier. High salt content (Class 8 and 9) was reached at all levels on the E.C. Row panels. Salt content belonging to class 10 was reached at levels 4 and 5. These results are compatible with visual observations. During the winter field visits, as the snow was melting, white salt lines were noticed on the panel at different levels. The tables show that there is a change in the salt content at a given level throughout the winter. One explanation is that the rain periodically washes out and redistributes the salt in the panel.

Table 5.5 gives the classes of salt content at the bottom of the E.C. Row panel for the degrees of saturation above 80%. It can be seen that 2 to 6% salt content was contained in the pore water of the panel. It is known that freeze-thaw cycles in the presence of a 3% salt solution produces the most severe scaling.

5.9 FREEZING AND MOISTURE CONTENT

As previous studies have indicated the extent of damage caused by freezing depends on the amount of moisture in the material. The moisture content and temperature data were studied to determine the degree of saturation of the concrete when the temperature fell below -3 C.

Although non-continuous temperature data were collected for the days when moisture readings were taken, the spot concrete temperature record indicates that at the E.C. Row site the concrete was subjected to numerous freeze-thaw cycles at fairly high degrees of saturation. The critical degree of saturation (that above which concrete is likely to be damaged by freezing) is about 80%. The degree of saturation at the bottom of the south facing panel E.C. Row barrier wall was well above 80% for sustained periods. It should be noted that the current readings were usually taken between noon and 2 p.m., which is usually the driest period of the day for the concrete. It can therefore be

assumed that higher moisture contents were reached at other times.

6.0 CONCLUSIONS AND RECOMMENDATIONS

The overall objective of this research project was to establish the microenvironment existing at the surface and within the concrete barrier walls through the winter months and to relate it to the ambient climate conditions.

To accomplish this, indirect methods of measurement of temperature, moisture, and salt conditions existing at and in the near sub-surface of the concrete were developed. It has been shown that the "capacitance effect" determined by measuring the current at 10Hz and 100Hz, can be used to determine the moisture content, and to some degree, the salt content of the concrete.

The temperature measurements indicated that the sun's rays can quickly raise the temperature of the concrete surface by over 10 degrees higher than the ambient. Thus, on a day when the air temperature is below freezing, the concrete surface can be well above freezing. The sub-surface temperature lags behind the surface temperature by several degrees. The surface can undergo several cycles of freezing and thawing during the day, especially on days when partly cloudy conditions exist. On such days, as soon as the cloud obscures the sun, the surface begins to cool rapidly and freeze.

The rapid temperature change at the concrete surface was documented. Also shown was the large difference in temperature possible between the surface and the sub-surface of the concrete under some climatic conditions. These changes and differences in temperature no doubt set up thermal stresses and contribute to the deterioration of the concrete.

The concrete panels were found to be in "critical" saturation conditions while undergoing freezing and thawing cycles. Also, the salt content of the surface and the near surface after only one winter of exposure was determined to be in the 2 to 6% range - a concentration recognized to be most harmful.

The orientation of the panels relative to the sun was found to have a major influence on the temperature extremes attained, on the rate of change of temperature, and on the wetting-drying frequency. South-facing panels underwent significantly larger changes in these parameters.

The shape of the panel had a bearing on the moisture and temperature conditions. The lower, curved portion was found to have higher, and more frequent changes in these parameters.

In summary, it can be concluded that south-facing panels experience a much harsher climatic environment than any other orientation.

REFERENCES

1. Bell, J.R., Leonards, G.A., Dolch, W.L., "Determination of moisture content of hardened concrete by its dielectric properties", ASTM Proc., vol. 63, 1963, pp. 997-1007

2. Spencer, R.W., "Measurement of the moisture content of concrete", J. of the ACI, vol. 34, 1937, pp. 45-61.

3. Hammond, E., Robson, T.D., "Comparison of electrical properties of various cements and concretes", The Engineer, 1955, Jan., pp. 78-80.

4. Wittington, H.W., McCarter, J., Forde, M.C., "The conduction of electricity through concrete", Mag. Con. Res., vol. 33, no. 114, March, 1981, pp. 48-60.

5. Ramachandran, V.S., "Calcium Chloride in concrete", Applied Science Publishers Ltd., London, 1976, 216 p.

TABLE 3.1

Results of chloride analysis for concrete of Composition E
(after saturation in given salt solution)

Salt Solution	% Chloride	STD*	CV**
1%	0.0815		
1%	0.0798	0.0090	1.05%
1%	0.0807		
4%	0.2134		
4%	0.2138	0.0013	0.61%
4%	0.2113		
8%	0.3557		
8%	0.3513	0.0028	0.78%
8%	0.3564		

*STD = standard deviation
** = coefficient of variation

TABLE 3.2

Multiple Linear Regression Model for Compositions A and B

	Composition A	Composition B
Degree of Saturation =	62.098	60.501
	+ 9.441 x L I100	+ 22.116 x L I100
	+ 11.597 x L I10	+ 2.764 x L I10
	+ 23.390 x I100	+ 17.906 x I100
R Square	0.858	0.847
Number of Observations	2066	2563
PR F	0.0001	0.0001

TABLE 3.3

Regression analysis model for salt content prediction.

	Composition A	Composition B
Salt Content =	- 0.612	3.875
	16.106 x CAP	126.502 x CAP
	1.981 x LCAP	5.558 x LCAP
	- 55.192 x I10	14.604 x I10
	43.870 x I100	- 40.883 x I100
	11.279 x LI10	16.854 x LI10
	- 15.230 x LI100	- 23.558 x LI100
	0.074 x DEGSAT	0.083 x DEGSAT
R-square	0.263	0.329
Number of Observations	2066	2563
FR F	0.0001	0.0001

TABLE 3.4

Calculated Salt Content Categories

Class	Range of degree of saturation (%)	Range of current I10 (MA)	Range of salt content in the solu- (%)	Expected salt in the concrete (%)
0	0 - 39.9	Any	0 - 9	0.033 - 0.379
	Any	0 - 0.19		
1	40 - 59.9	0.2 - 0.6	0 - 9	0.033 - 0.379
2	60 - 79.9	0.2 - 0.6	0 - 9	0.033 - 0.379
3	60 - 79.9	0.6 - 1.0	1 - 9	0.072 - 0.379
4	60 - 79.9	1.0 - 1.4	2 - 6	0.110 - 0.264
5	60 - 79.9	1.4 - 1.8	5	0.226
6	80 - 100	0.2 - 0.6	0 - 1	0.033 - 0.072
7	80 - 100	0.6 - 1.0	1 - 3	0.072 - 0.149
8	80 - 100	1.0 - 1.4	2 - 6	0.110 - 2.64
9	80 - 100	1.4 - 1.8	5 - 9	0.226 - 0.379
10	80 - 100	1.8 - 2.2	5 - 9	0.266 - 0.379

TABLE 4.1

Current and moisture data from the samples chiseled from the roof and E.C. Row panels

Specimen	Weight (g)	DEGSAT (%)	Current (mA) SURFACE I10	SURFACE I100	INSIDE I10	INSIDE I100	Location in panel	Conc. Temp (oC)	Date	Time
E1	1.33	63.3	0.307	0.345	0.455	0.481	Top	5	Mar.20	12:16
E2	1.42	60.0	0.304	0.344	0.372	0.422	Middle	5	Mar.20	12:16
E3	1.91	80.0	0.469	0.538	0.394	0.461	Bottom	5	Mar.20	12:16
E4	4.49	50.0	0.145	0.164	0.266	0.318	Bottom	20	Jul. 1	6:30
E5	3.35	45.0	0.132	0.148	0.123	0.148	Bottom	20	Jul. 1	6:30
E6	1.20	48.8	0.123	0.128	0.228	0.261	Middle	20	Jul. 1	6:30
E7	5.71	57.7	-	-	0.138	0.170	Bottom	20	Jul. 1	6:30
R1	2.37	48.5	0.213	0.240	0.179	0.209	Bottom	18	Jul. 5	7:00
R2	5.65	54.0	0.117	0.127	0.142	0.163	Middle	18	Jul. 5	7:00
R3	2.42	41.5	0.149	0.164	0.096	0.109	Top	18	Jul. 5	7:00
R4	3.55	59.5	0.007	0.008	0.170	0.188	Bottom	18	May 17	11:00
R5	4.00	83.8	0.007	0.008	0.170	0.188	Bottom	18	May 17	11:00
R6	1.36	50.0	0.007	0.008	0.170	0.188	Bottom	18	May 17	11:00

TABLE 5.2

Frequency of Temperature Change in the E.C. Row Panel for the month of March

Thermo-couple	Rate of Cooling (C/h)						Rate of Warming (C/h)				
	18-15	15-12	12-9	9-6	6-3	3-0	0-3	3-6	6-9	9-12	12-15
1		1.2	0.0	7.1	4.7	87.1	89.6	4.7	4.7	0.0	0.9
2		1.1	0.0	5.5	6.6	86.8	89.0	5.0	5.0	0.0	1.0
3		1.1	0.0	6.7	4.5	87.6	89.3	4.9	3.9	1.0	1.0
4			1.1	4.5	5.6	88.8	88.2	6.9	2.9	1.0	1.0
5	1.1	1.1	1.1	5.6	5.6	85.6	88.1	6.9	2.0	2.0	1.0
6				2.3	9.1	88.6	91.3	6.8	1.0	1.0	
7				1.1	8.5	90.5	90.7	7.2	1.0	1.0	
8				2.2	6.7	91.1	91.1	5.9	2.0	1.0	
9				5.8	8.1	86.0	89.5	4.8	3.8	1.0	1.0
10				5.5	8.8	85.7	89.9	5.1	3.0	2.0	1.0
11				6.6	6.6	86.8	90.0	5.0	3.0	1.0	1.0
12				5.6	6.7	87.8	90.5	5.0	2.0	2.0	1.0
13				4.6	10.3	85.1	89.4	5.8	1.9	1.9	1.0
14				1.1	5.6	93.3	93.0	6.0	1.0		
15				3.2	4.3	92.5	93.9	3.1	3.1		
16				1.1	10.1	88.8	95.1	2.0	2.0	1.0	
17			1.2	3.6	8.4	86.7	91.7	5.6	2.8		
18				2.2	4.3	93.5	92.8	5.2	2.1		
Air					1.0	99.0	100				

TABLE 5.3

Cooling and Warming Rate Frequency (in %) for the Period of March 4 to March 24
E.C.Row Panel

Thermocouple	Rate of Cooling (C/h)				Rate of Warming (C/h)					
	12-9	9-6	6-3	3-0	0-3	3-6	6-9	9-12	12-15	15-18
1	0	0.7	3.7	96.6	94.9	2.2	2.9	0	0	0
6	0	0	0	100	83.9	12.1	4.0	0	0	0
5	0	0	1.5	98.5	89.7	9.7	0.6	0.6	0	0
10	0	0.7	2.9	96.4	89.6	9.7	0.6	0	0	0
22	0	0.8	1.5	97.7	94.2	4.6	1.3	0	0	0
14	0	0	2.0	98.0	96.6	2.9	0.6	0	0	0
19	0	0	3.4	96.6	93.9	4.8	1.2	0	0	0

TABLE 5.4

Average Degree of Saturation for the Roof Panels

Date March	Time h	1 cm Depth		Surface	
		South Facing	North Facing	South Facing	North Facing
6	14:20	53.3	49.9	0.0	13.1
10	0.00	85.0	74.0	71.2	63.6
11	13:40	68.9	60.0	36.5	30.4
12	10:50	62.3	56.7	28.1	30.02
13	13:20	65.5	50.0	30.5	21.8
14	8:35	69.8	63.2	44.3	34.2
18	16:40	50.3	48.8	0.0	13.9
27	10:35	30.2	31.5	0.0	0.0

TABLE 5.5

Categories of salt content for the bottom part of E.C. Row panel

Date	Level	1 cm Depth		Surface	
		DEGSAT	CLASS	DEGSAT	CLASS
26/1	6	87.2	9	82.7	8
28/1	6	83.8	8	--	-
11/2	6	81.0	8	--	-
11/2	7	81.3	8	80.9	8
11/2	8	85.9	9	82.8	8

Class 8 DEGSAT: 80-100%; I10: 1.0-1.4 mA; % salt: 2-6%

Class 9 DEGSAT: 80-100%; I10; 1.4-1.8 mA: % salt: 5-9%

TABLE 5.6

Average Degree of Saturation
for the North and the South Facing Roof Panels

Date March	Time h	1 cm depth South Facing	1 cm depth North Facing	Surface South Facing	Surface North Facing
6	14:20	53.3	49.9	0.0	13.1
10	0.00	85.0	74.0	71.2	63.6
11	13:40	68.9	60.0	36.5	30.4
12	10:50	62.3	56.7	28.1	30.02
13	13:20	65.5	50.0	30.5	21.8
14	8:35	69.8	63.2	44.3	34.2
18	16:40	50.3	48.8	0.0	13.9
27	10:35	30.2	31.5	0.0	0.0

TABLE 5.7

Salt content categories in the Bottom Part of E.C. Row Panel

Date	Level	1 cm depth		Surface	
		DEGSAT	CLASS	DEGSAT	CLASS
26/1	6	87.2	9	82.7	8
28/1	6	83.8	8	--	-
11/2	6	81.0	8	--	-
11/2	7	81.3	8	80.9	8
11/2	8	85.9	9	82.8	8

Class 8 DEGSAT: 80-100%; I10: 1.0 %

Class 9 DEGSAT: 80-100%; I10; 1.4-1.8 mA: % salt: 5-9%

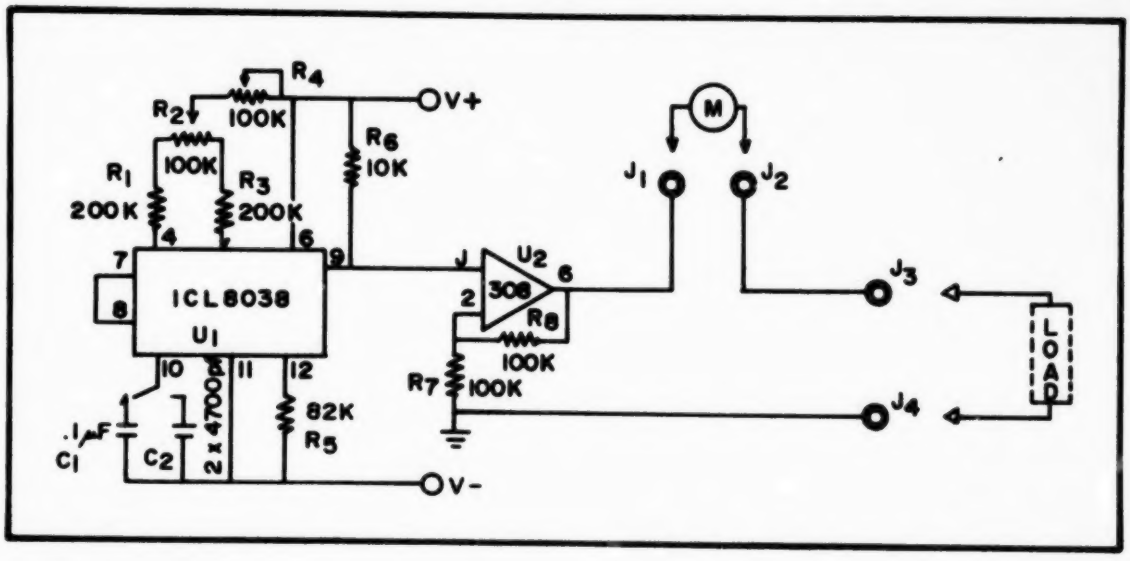

2.2.1/ Square Wave Generator

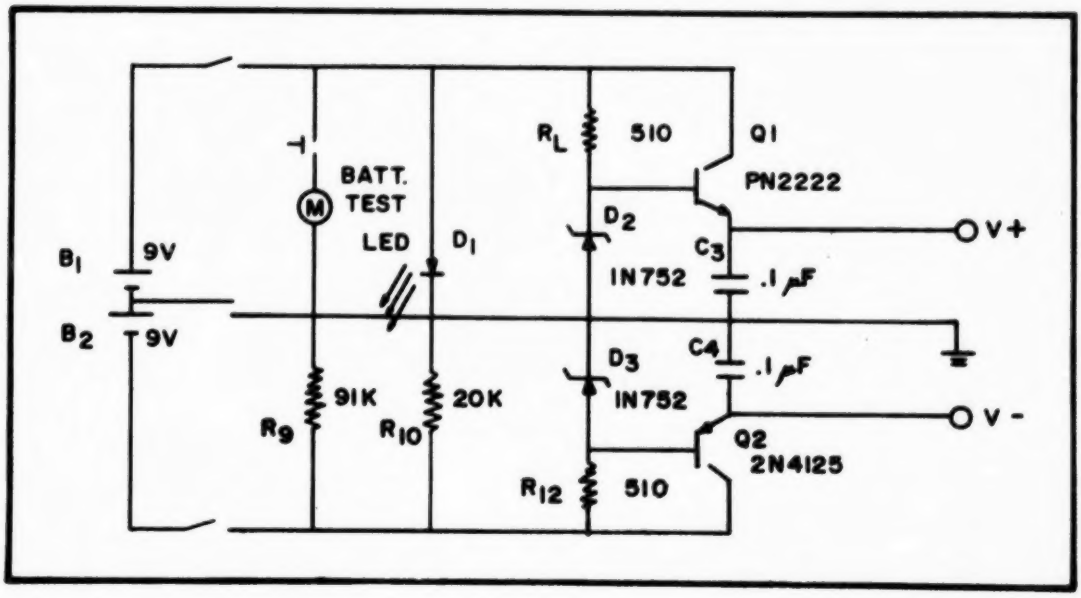

2.2.2/ Regulated DC Power Source Circuit

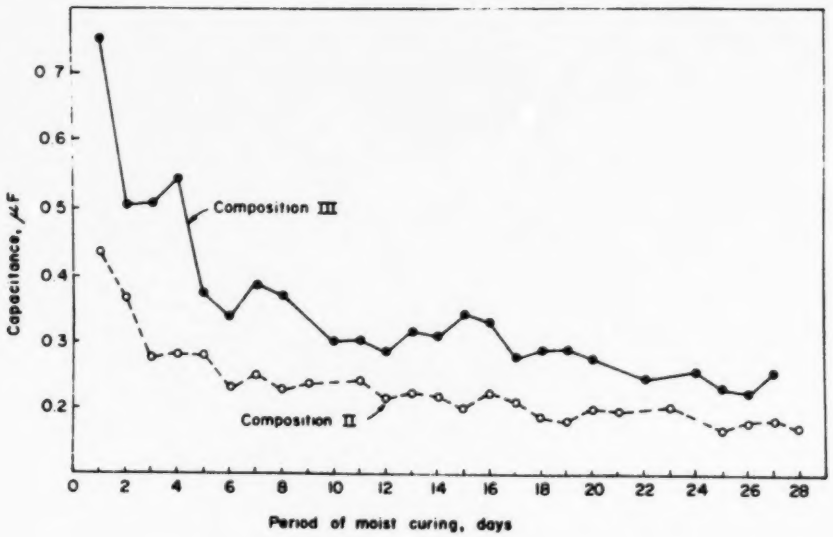

3.1/ Change of Capacitance with Time for Two W/C

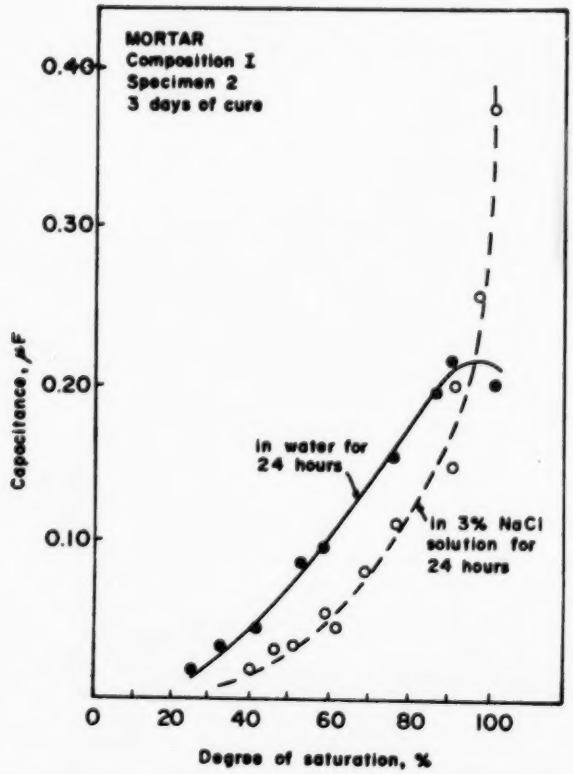

3.2/ Effect of Salt on the Capacitance Effect

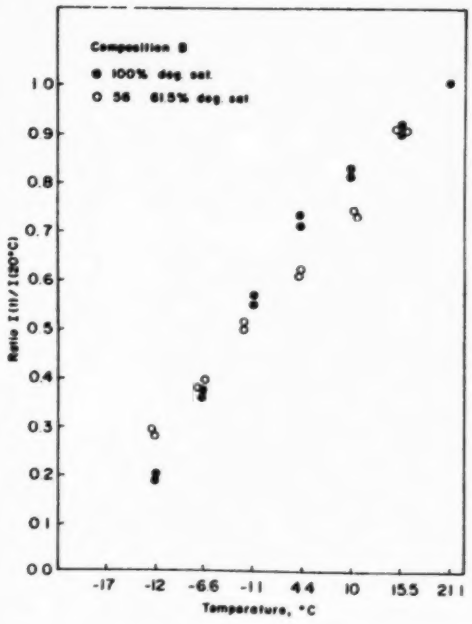

3.3/ Effect of Temperature on the September 20 Reading

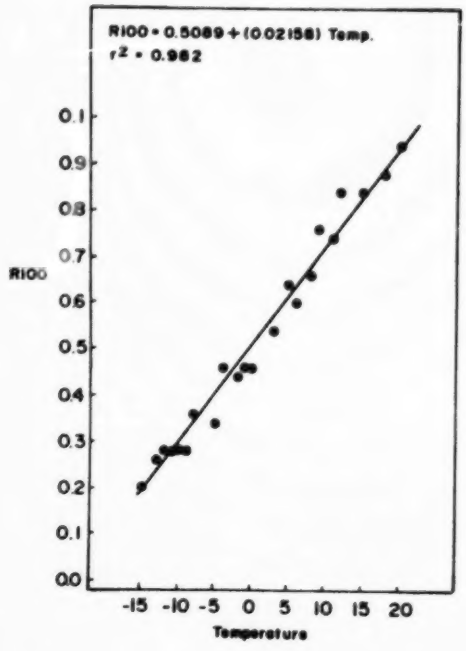

3.4/ Current Ratio I(T)/I(20) vs Temperature at 100 Hz

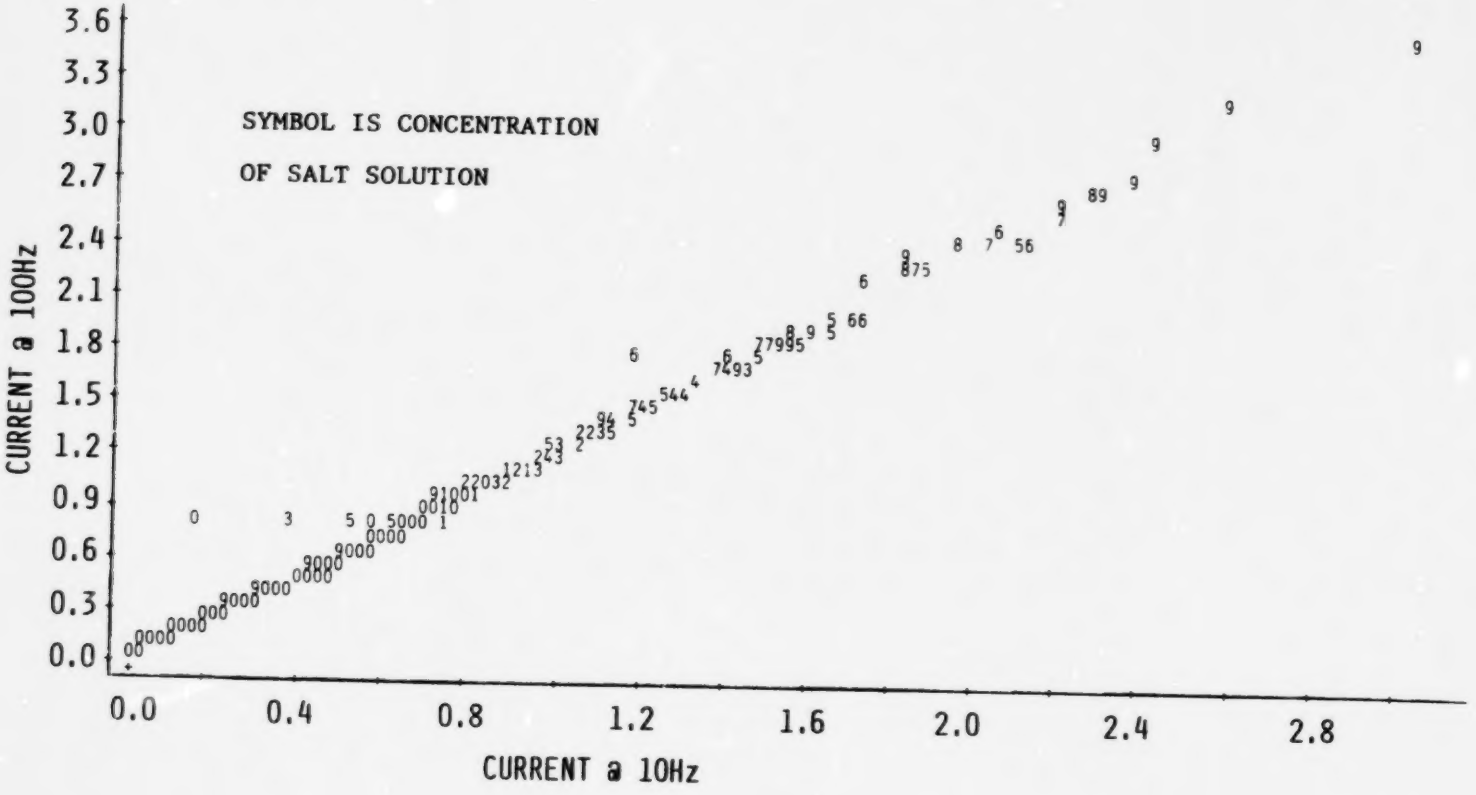

3.5/ Current at 10 Hz vs Current at 100 Hz, Composition E

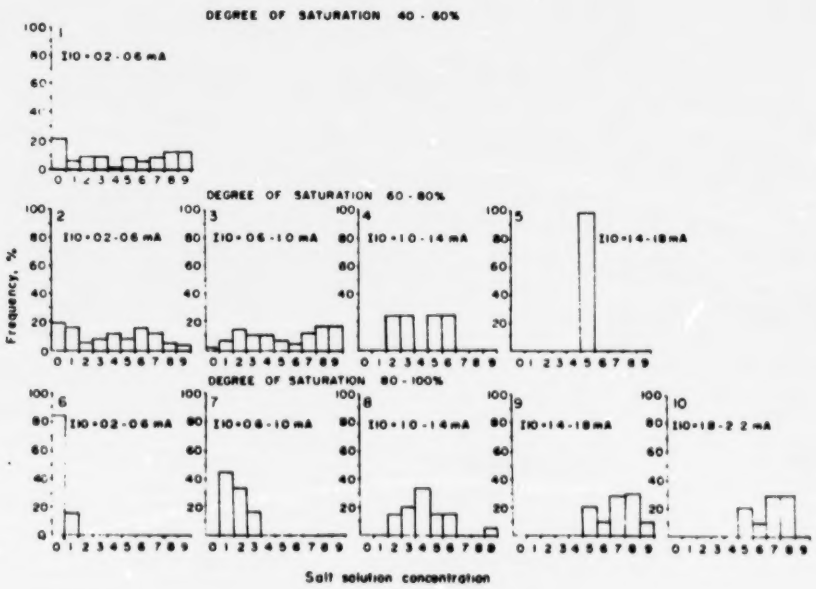
DEGREE OF SATURATION 40 - 60%
I10 = 02 - 06 mA
DEGREE OF SATURATION 60 - 80%
I10 = 02 - 06 mA
I10 = 06 - 10 mA
I10 = 10 - 14 mA
I10 = 14 - 18 mA
DEGREE OF SATURATION 80 - 100%
I10 = 02 - 06 mA
I10 = 06 - 10 mA
I10 = 10 - 14 mA
I10 = 14 - 18 mA
I10 = 18 - 2 2 mA
Frequency, %
Salt solution concentration

3.6/ Frequency of Occurrence of Current Readings at 10 Hz for Three Ranges of Degree of Saturation

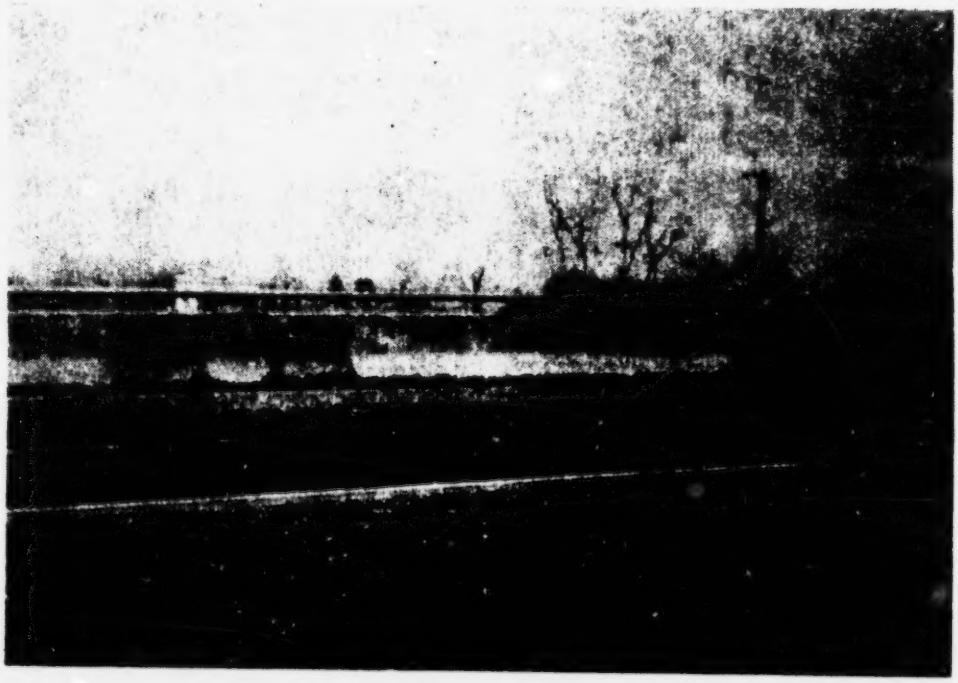

4.1/ General View of the E.C. Row Site

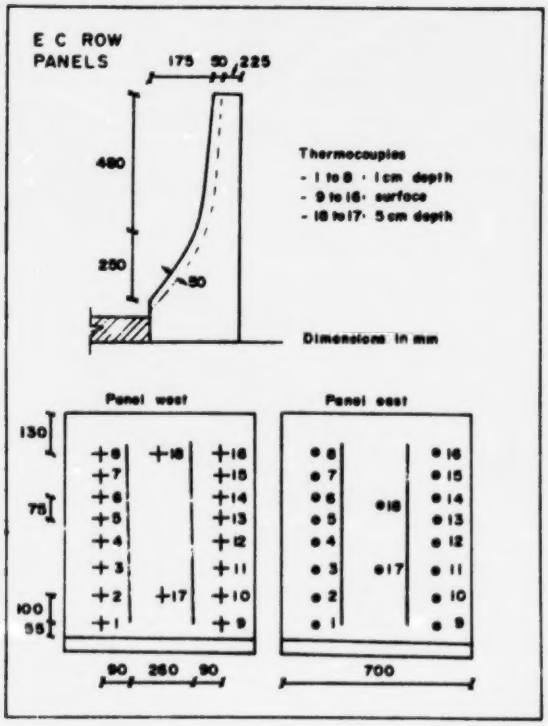

4.2/ Location of the Thermocouples in the E.C. Row Panels

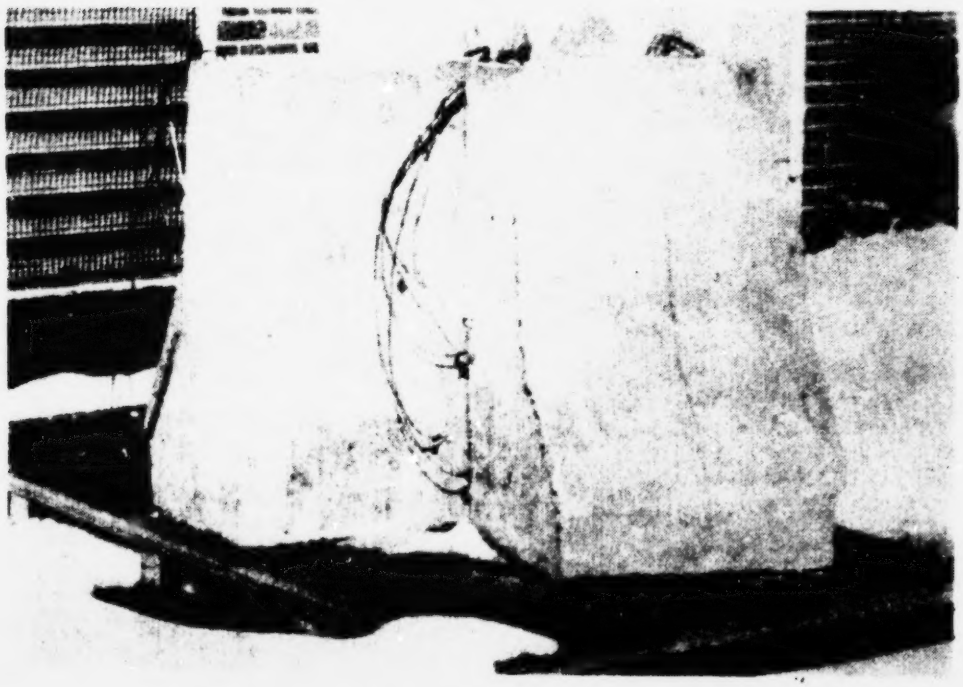

4.3/ General View of Roof Installation

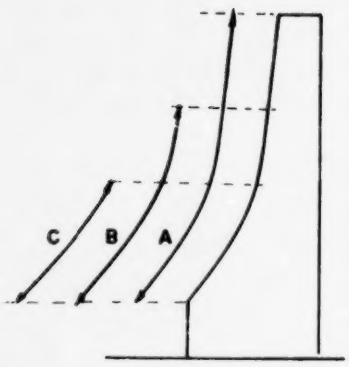

A : sprayed on May 20
B : sprayed on June 2
C : sprayed on June 6

4.4/ Schematic Diagram Showing How the Roof Panel was Sprayed With a Salt Solution

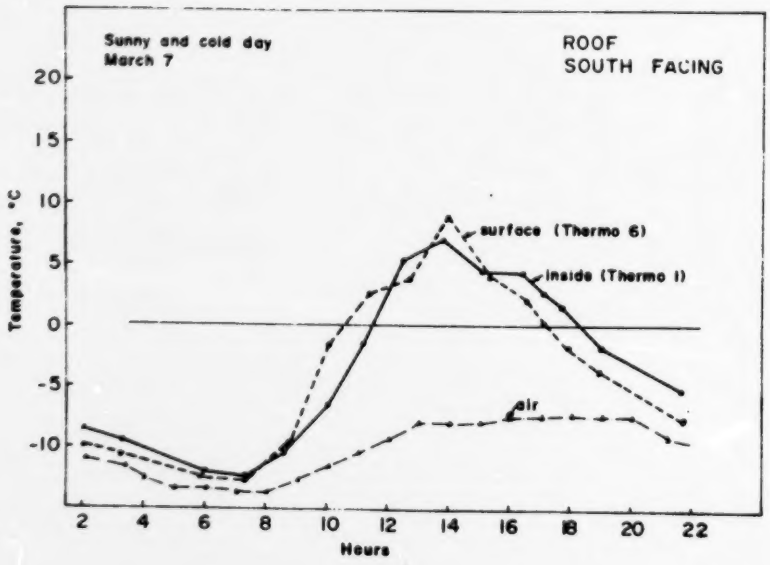

5.1/ Typical Temperature Variation in the Roof's South Facing Panel for a Sunny, Cold Day

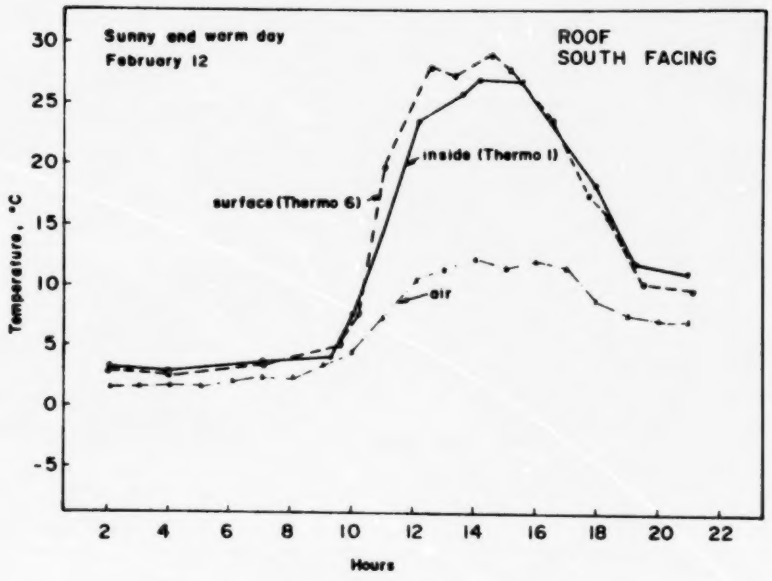

5.2/ Typical Temperature Variation in the Roof's South Facing Panel for a Sunny, Warm Day

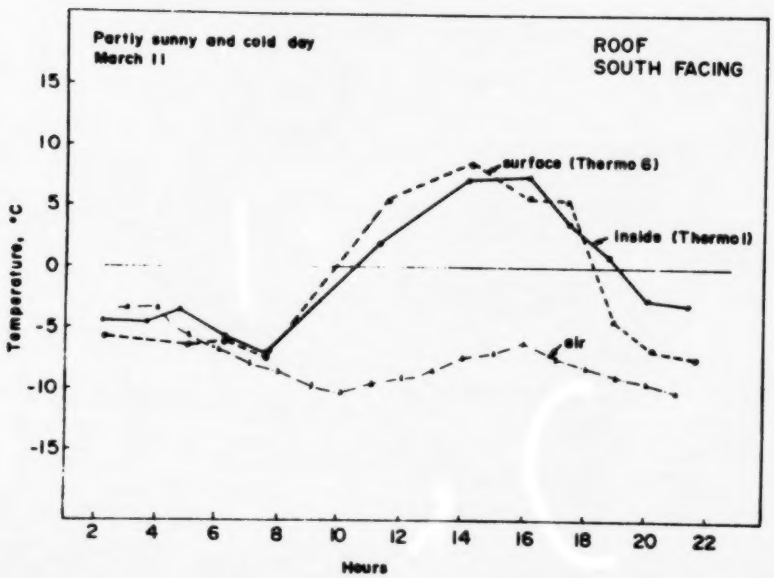

5.3/ Typical Temperature Variation in the Roof's South Facing Panel for a Partly Sunny, Cold Day

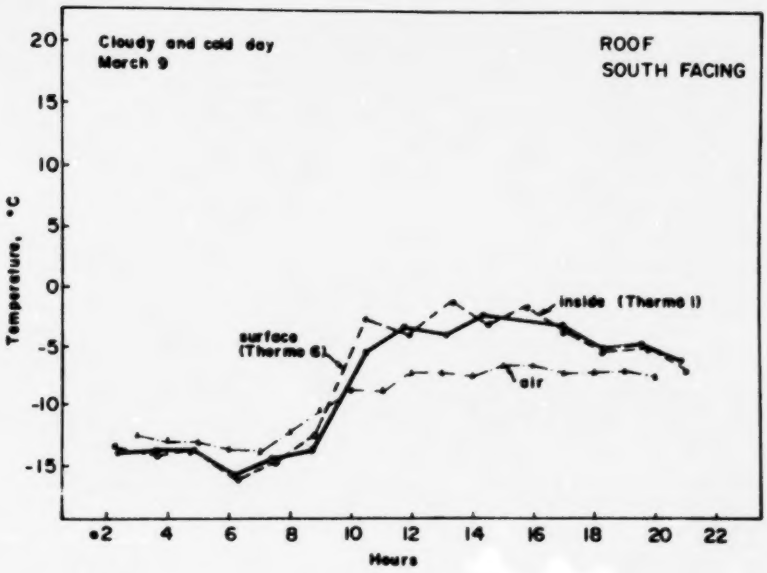

5.4/ Typical Temperature Variation in the Roof's South Facing Panel for a Cloudy, Cold Day

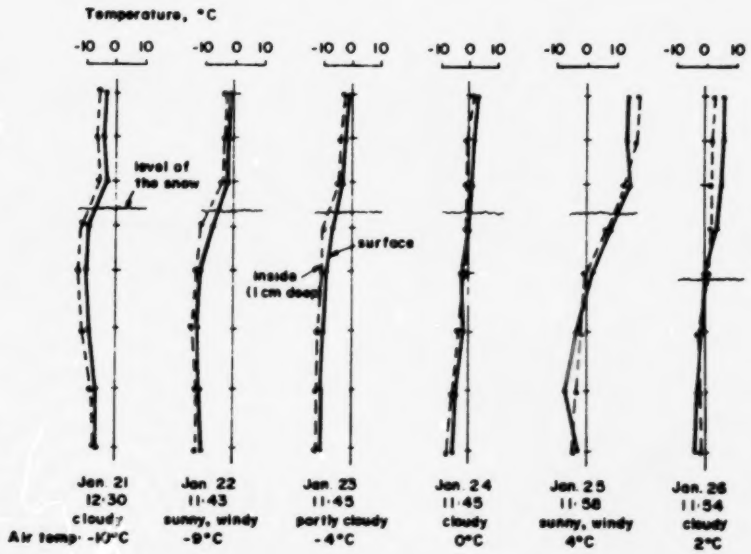

5.5/ Temperature Distribution in Panel East (E.C. Row), from January 21 to January 26, 1984

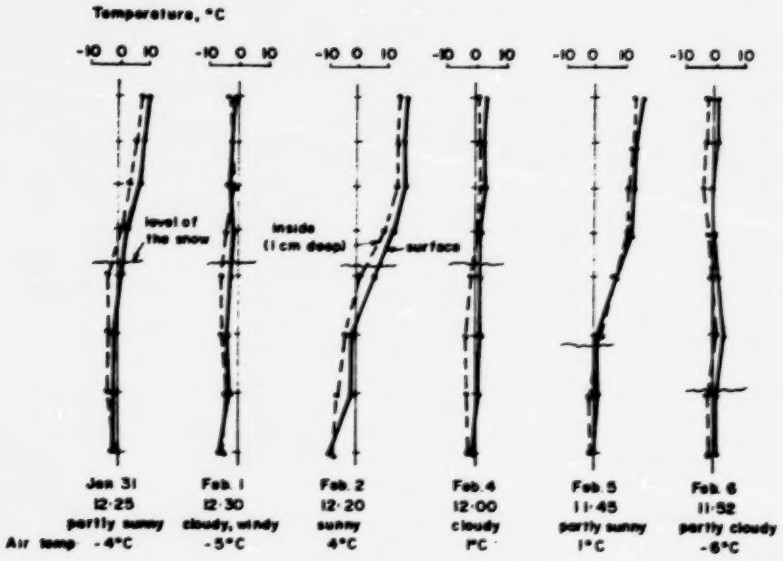
Temperature, °C
-10 0 10
level of the snow
inside (1 cm deep)
surface
Jan 31 12:25 partly sunny
Feb. 1 12:30 cloudy, windy
Feb. 2 12:20 sunny
Feb. 4 12:00 cloudy
Feb. 5 11:45 partly sunny
Feb. 6 11:52 partly cloudy
Air temp -4°C -5°C 4°C PC 1°C -6°C

5.6/ Temperature Distribution in Panel East (E.C. Row), from January 31 to February 6, 1984

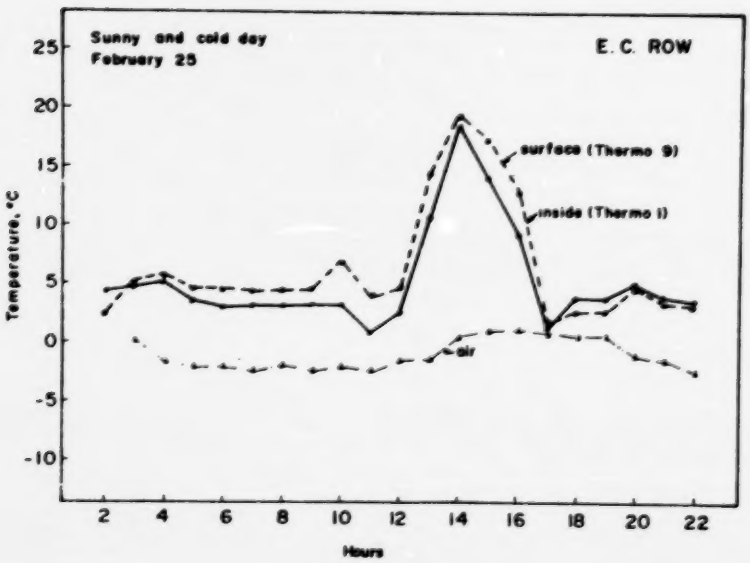

5.7/ Daily Temperature Variation for Panel West (E.C. Row), on February 25, 1984

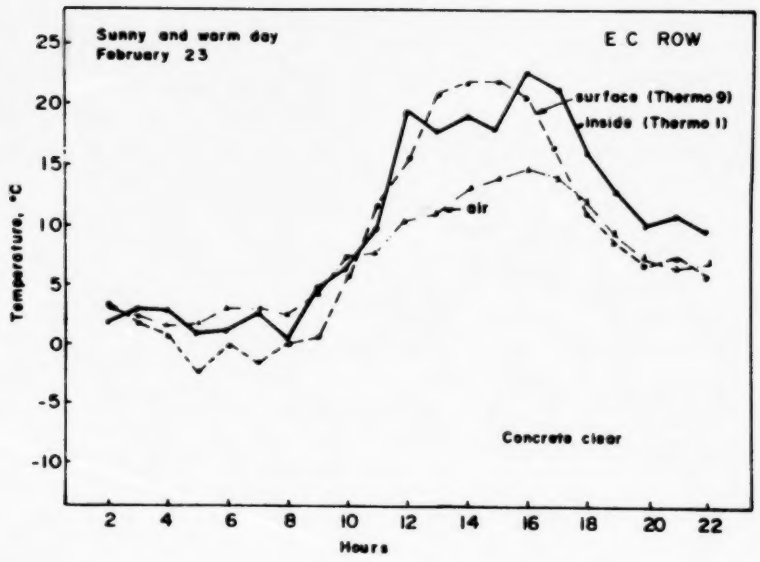

5.8/ Daily Temperature Variation for Panel West (E.C. Row), on February 23, 1984

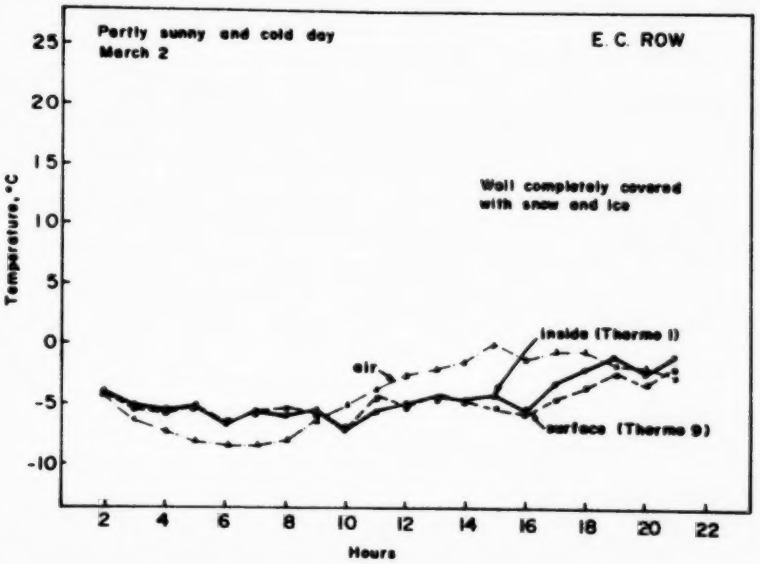

5.9/ Daily Temperature Variation for Panel West on March 2, 1984

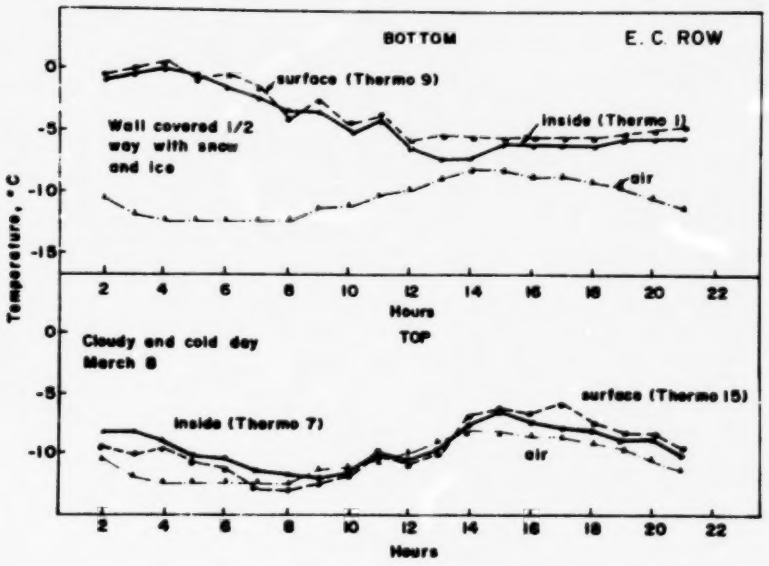

5.10/ Daily Temperature Variation for Panel West on March 8, 1984

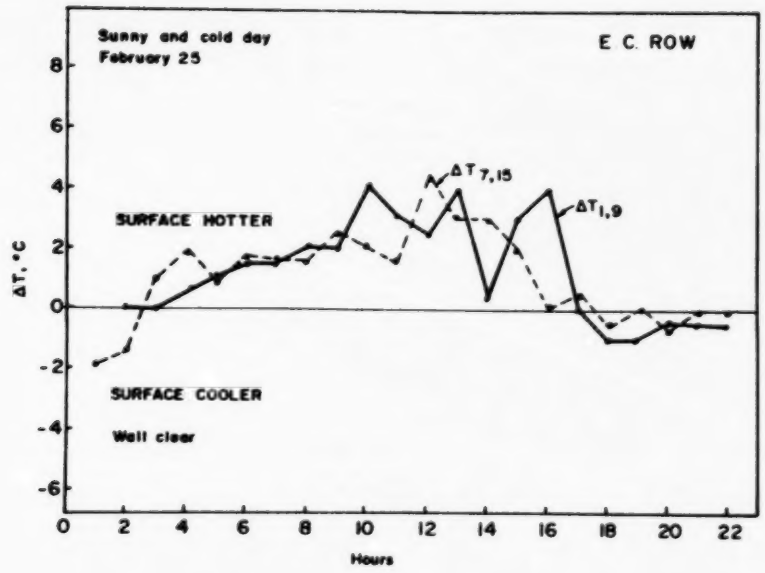

5.11/Typical Change in Δ T for February 25, 1984

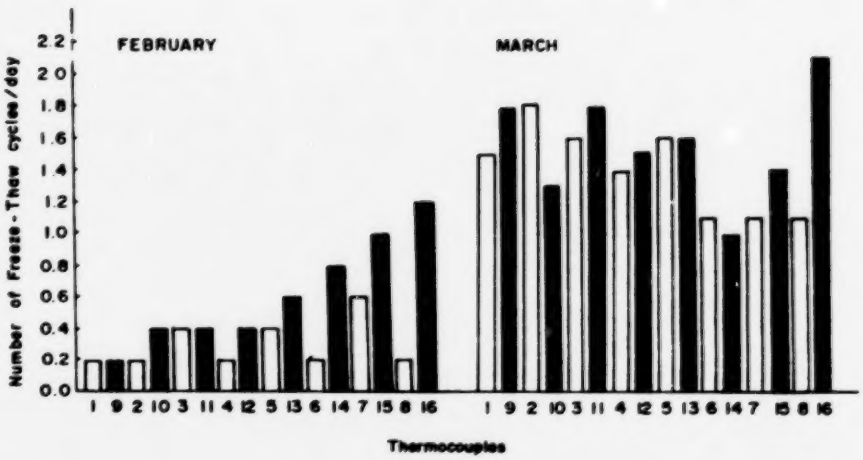

5.12/ Typical Change in Δ T for March 7, 1984

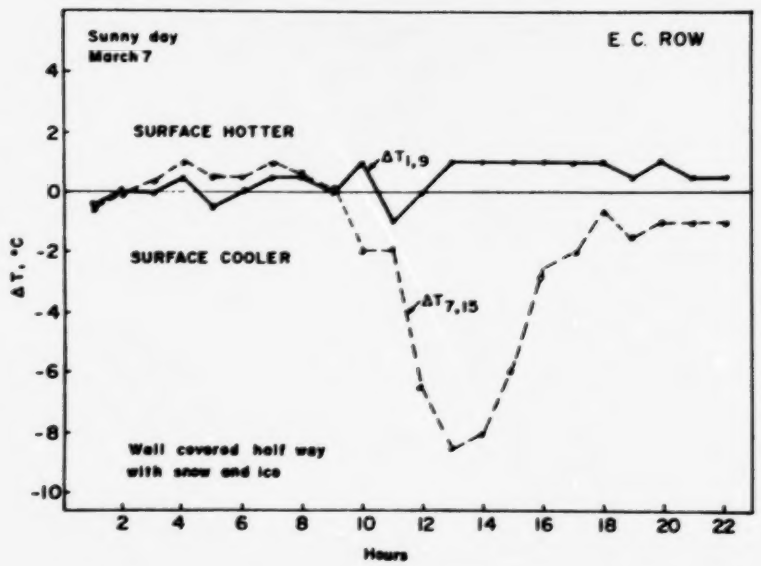

5.13/ Number of Freezing and Thawing Cycles Per Day for all the Thermocouples

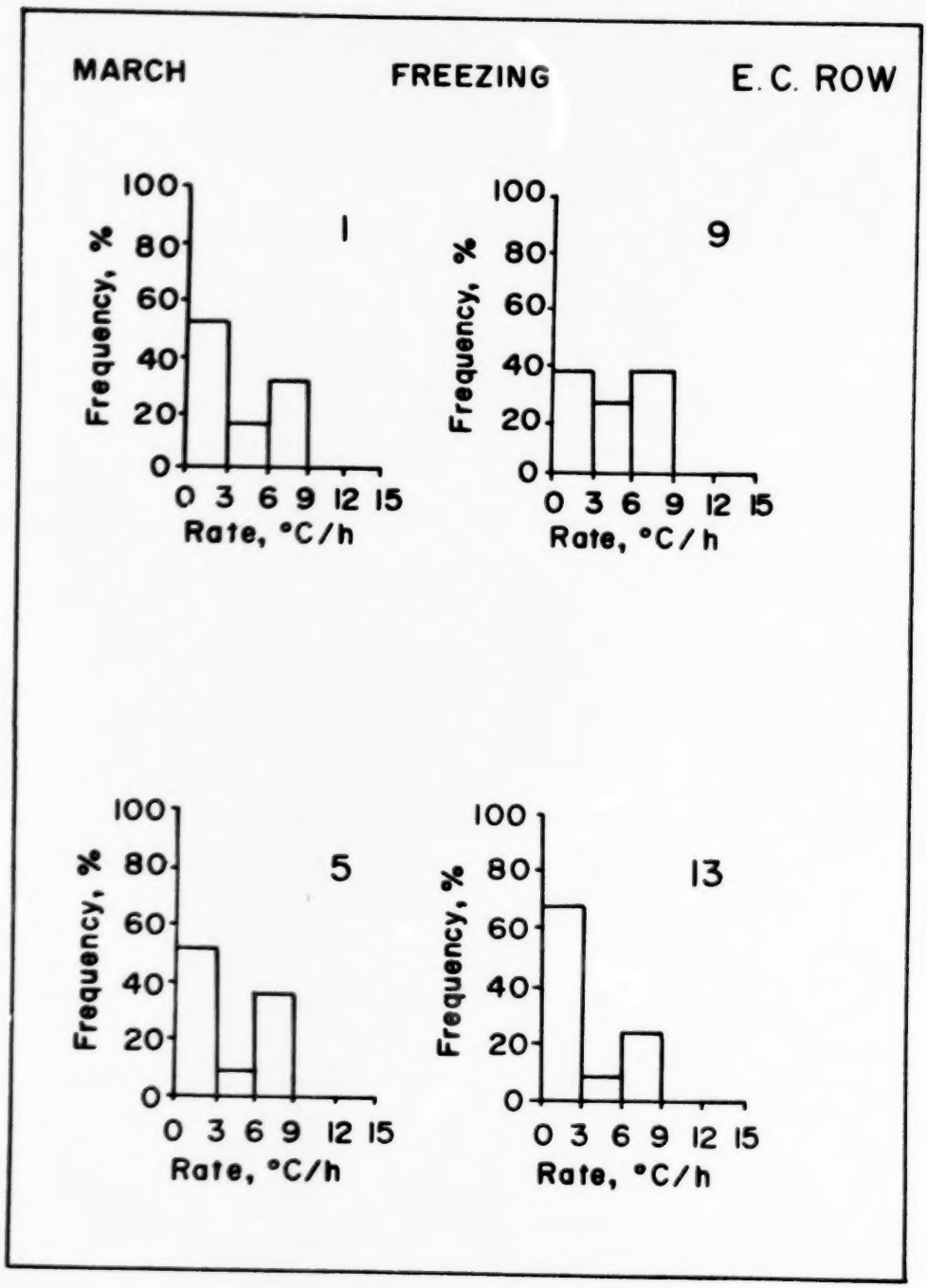

5.14/ Frequency of Freezing Rate for Thermocouples 1, 9, 5, and 13, for the Month of March

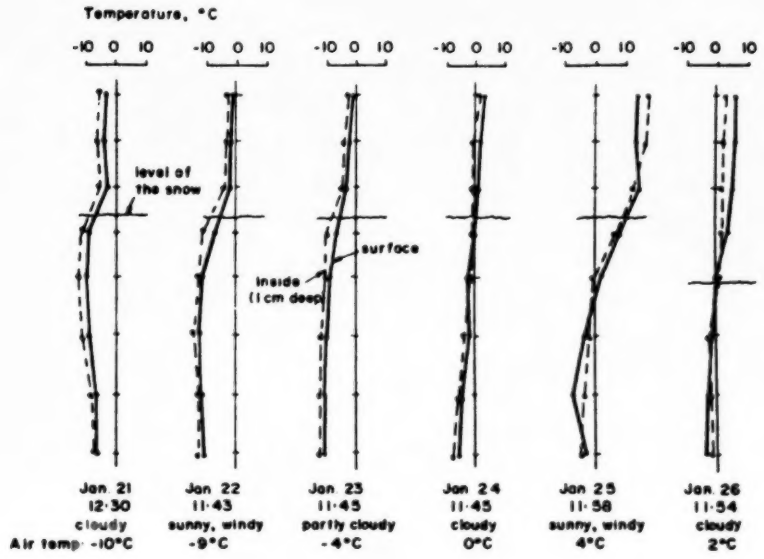
Temperature, °C
-10 0 10
level of the snow
surface
inside (1 cm deep)
Jan 21 12·30 cloudy Air temp: -10°C
Jan 22 11·43 sunny, windy -9°C
Jan 23 11·45 partly cloudy -4°C
Jan 24 11·45 cloudy 0°C
Jan 25 11·58 sunny, windy 4°C
Jan 26 11·54 cloudy 2°C

5.15/ Temperature Distribution in Panel East Installed on E.C. Row, from January 21 to January 26, 1984

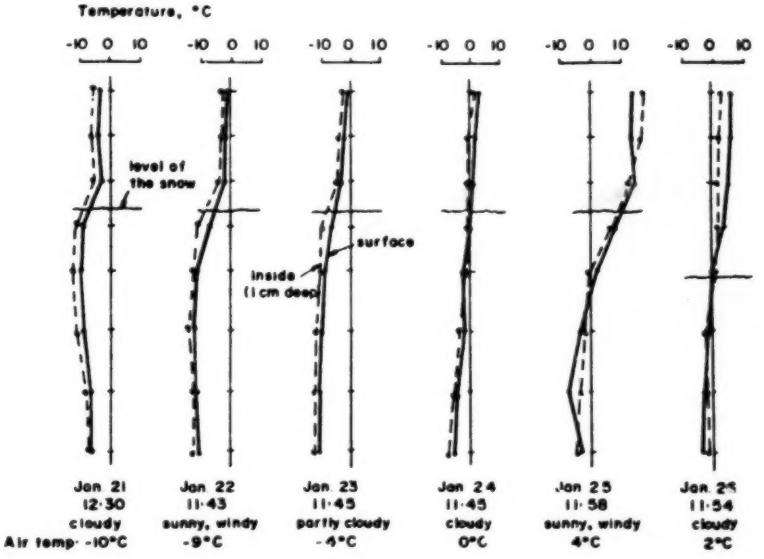
Temperature, °C
-10 0 10
level of the snow
surface
inside (1 cm deep)
Jan 21 12·30 cloudy Air temp: -10°C
Jan 22 11·43 sunny, windy -9°C
Jan 23 11·45 partly cloudy -4°C
Jan 24 11·45 cloudy 0°C
Jan 25 11·58 sunny, windy 4°C
Jan 26 11·54 cloudy 2°C

5.16/ Temperature Distribution in Panel East Installed on E.C. Row, from January 31 to February 6, 1984